Ensemble Simulation of Twenty-First Century Climate Changes: Business-as-Usual versus CO_2 Stabilization

Aiguo Dai, Gerald A. Meehl, Warren M. Washington, Tom M. L. Wigley, and Julie M. Arblaster
National Center for Atmospheric Research,* Boulder, Colorado

ABSTRACT

Natural variability of the climate system imposes a large uncertainty on future climate change signals simulated by a single integration of any coupled ocean–atmosphere model. This is especially true for regional precipitation changes. Here, these uncertainties are reduced by using results from two ensembles of five integrations of a coupled ocean–atmosphere model forced by projected future greenhouse gas and sulfate aerosol changes. Under a business-as-usual scenario, the simulations show a global warming of ~1.9°C over the twenty-first century (continuing the trend observed since the late 1970s), accompanied by a ~3% increase in global precipitation. Stabilizing the CO_2 level at 550 ppm reduces the warming only moderately (by ~0.4°C in 2100). The patterns of seasonal-mean temperature and precipitation change in the two cases are highly correlated ($r \approx 0.99$ for temperature and $r \approx 0.93$ for precipitation). Over the midlatitude North Atlantic Ocean, the model produces a moderate surface cooling (1°–2°C, mostly in winter) over the twenty-first century. This cooling is accompanied by changes in atmospheric lapse rates over the region (i.e., larger warming in the free troposphere than at the surface), which stabilizes the surface ocean. The resultant reduction in local oceanic convection contributes to a 20% slowdown in the thermohaline circulation.

1. Introduction

As the world economy and population grow in the twenty-first century, atmospheric concentrations of CO_2 and other greenhouse gases are likely to continue to rise (Nakićenović and Swart 2000). Credible projections of future climate changes induced by these increases have many practical applications (e.g., for climate impact assessments and to guide future emissions controls). Most previous simulations of such changes using coupled ocean–atmosphere general circulation models (GCMs; Manabe et al. 1991; Cubasch et al. 1992; Mitchell et al. 1995; Roeckner et al. 1999; Russell and Rind 1999; Boer et al. 2000; Meehl et al. 2000a,b; Dai et al. 2001a) have been carried out using a single realization for each emissions scenario. However, it is well-known that individual realizations show considerable differences from run to run (e.g., Delworth and Knutson 2000), since each run includes its own specific realization of the model's internal variability. These differences cause uncertainties in model-simulated climate changes that are in addition to uncertainties associated with a model's climate sensitivity and other intermodel differences (Allen et al. 2000) and with future emissions (Kattenberg et al. 1996). While areal and temporal averaging can partly reduce uncertainties related to internal variability, intraensemble differences can still make climate changes on regional ($L \sim 10^3$ km) and smaller scales from single realizations noisy and irreproducible (Dai et al. 2001a).

The preferred solution to this problem is to carry out multiple realizations (an ensemble) for each emissions case (starting from different initial conditions), and to average these. Ensembles have been used in climate studies with GCMs (e.g., Cubasch et al. 1994; Zwiers 1996; Hansen et al. 1997; Rowell 1998; Delworth and Knutson 2000; Wehner 2000; Stott et al. 2000, 2001). Most previous work, however, has employed only relatively short ensemble simulations or

*The National Center for Atmospheric Research is sponsored by the National Science Foundation.
Corresponding author address: Dr. Aiguo Dai, National Center for Atmospheric Research, P.O. Box 3000, Boulder, CO 80307.
E-mail: adai@ucar.edu
In final form 16 May 2001

has focused on ensemble variability (relative to signal) rather than on the prediction of future climate changes under likely future emissions scenarios. An exception is the recent study by Mitchell et al. (2000) who applied a coupled GCM (HadCM2) to examine the effect of stabilizing atmospheric CO_2 on global and regional climate changes. These authors used, as an idealized baseline, an ensemble of four integrations under a 1% yr^{-1} CO_2 increase (with no sulfate aerosol or other greenhouse gas forcings) and compared these results with single integrations under two different CO_2 stabilization scenarios.

Here, we present results from two ensembles of five integrations of a coupled ocean–atmosphere GCM forced with projected concentrations of greenhouse gases and sulfate aerosols for the twenty-first century. We use a realistic business-as-usual (BAU) scenario as the baseline and compare this with a CO_2 stabilization (STA550) scenario (the scenario details are given in Dai et al. 2001a). Our study differs from previous studies in the following ways: we use ensemble integrations for both the BAU and STA550 cases, we include a full range of greenhouse gas changes in our scenarios together with sulfate aerosol effects, and we use a model in which there are no artificial flux adjustments.

2. Model, emissions scenarios, and experiments

The coupled ocean–atmosphere model used here is the Parallel Climate Model (PCM; Washington et al. 2000). The PCM is global in domain and consists of an atmospheric GCM (T42 truncation, ~2.8° lat/long resolution, with 18 vertical layers), an ocean GCM (~2/3° average resolution with 32 vertical layers), a land surface model, and a sea-ice model. The PCM does not use flux adjustments. It produces a stable climate (except for the deep oceans where there is a small cooling with time) under current conditions that is comparable to observations (Washington et al. 2000; Dai et al. 2001b) and has near-observed El Niño amplitude and spatial patterns (Meehl et al. 2001).

The development of the two future scenarios (BAU and STA550) of greenhouse gas (CO_2, CH_4, N_2O, O_3, and CFCs) concentrations and SO_2 emissions is described in Dai et al. (2001a). The two scenarios were designed to be a "matched" pair. The only difference between the two scenarios is in the CO_2 concentration: the CO_2 increase rate is substantially lower under the STA550 scenario and CO_2 concentrations are projected to stabilize at 550 ppm in 2150 following Wigley et al. (1996). Internally consistent emissions for CO_2 and SO_2 were generated (under the BAU scenario) using an energy-economics model (Edmonds et al. 1997) driven by regionally specific assumptions with regard to population growth, economic growth, energy use per capita, technology development, etc. The CO_2 level in the year 2100 is ~710 ppm in the BAU case (which is similar to the average of all concentration projects under the Intergovernmental Panel on Climate Change's (IPCC) Special Report on Emissions Scenarios (SRES) no-intervention-policy emissions scenarios (Naki enovi and Swart 2000) and is ~540 ppm under the STA550 scenario. Global SO_2 emissions peak around 2005 (at 81 Tg S yr^{-1}, 1 Tg = 10^{12} g) and then decline steadily until 2080 when they stabilize at ~30 Tg S yr^{-1}. These SO_2 emissions lie well within the range of SO_2 emissions in the SRES scenarios (Nakićenović and Swart 2000). Atmospheric sulfate loadings under the SO_2 emissions were taken from earlier simulations using the National Center for Atmospheric Research (NCAR) Climate System Model (CSM); (Dai et al. 2001a). Our BAU scenario, which was developed before the IPCC SRES scenarios were available, is close to the average behavior of all SRES scenarios.

The simulations started from 1870 using different conditions obtained from a coupled spinup integration for each ensemble run and were integrated through 1999 using greenhouse gas concentrations and sulfate loadings based on observations (Dai et al. 2001b). The climate conditions at the end of the historical simulations are comparable to recent observations. The simulations were extended into the twenty-first century using the projected greenhouse gas concentrations. A 230-yr control run with trace gas concentrations appropriate for 1870 was also completed. Two 5-member ensembles of runs from 1870 to 2099 were used to derive the ensemble mean and ensemble range for the historical, BAU, and STA cases. The ensemble range was defined as the largest value minus the smallest value in the ensemble at each year. For a Gaussian process, this minimum-to-maximum range is 2.475 times the standard deviation for 5-member ensembles.

3. Temperature and ocean circulation changes

Figure 1 shows the ensemble mean and range for globally averaged, annual-mean surface air tempera-

ture. For the twentieth century, the rapid warming since the late 1970s was simulated well whereas the warming around 1940 was not captured by any of the model runs. Increasing the number of the ensemble runs to 10 for the twentieth century also failed to capture the peak warming around 1940. This is in contrast to an earlier study (Delworth and Knutson 2000), which found that 1 of 5 ensemble runs using the Geophysical Fluid Dynamics Laboratory (GFDL) model forced with greenhouse gases and sulfate reproduced both the peak warming around 1940 and the warming after the late 1970s. Adding solar forcing (i.e., changing the solar irradiance based on observations) in our experiments produced much better agreement between the observed and simulated twentieth century global-mean temperature (Meehl et al. 2001, manuscript submitted to *J. Climate*).

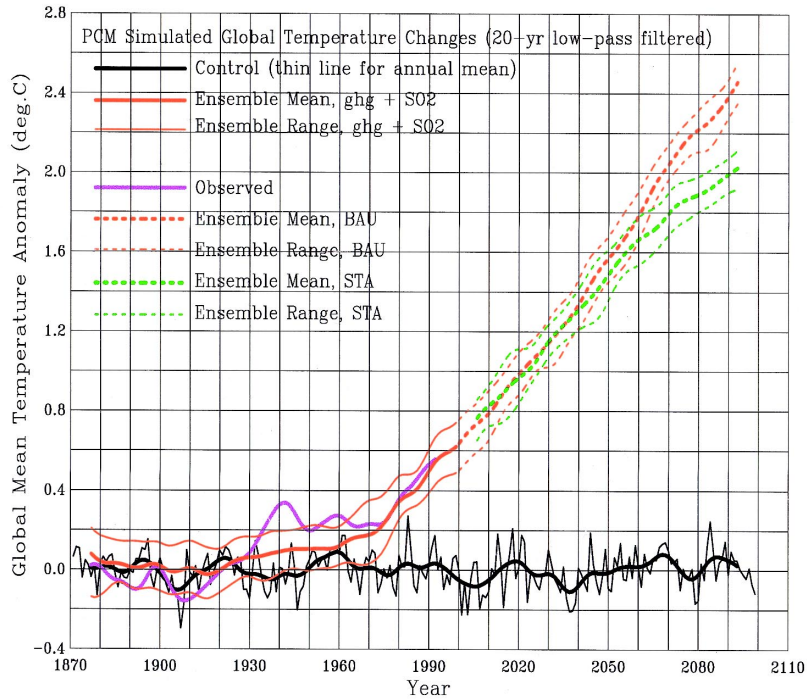

FIG. 1. Globally averaged, annual-mean surface air temperature change from 1870 to 2099 simulated by the PCM under the historical greenhouse gas and sulfate aerosol forcing (red solid curves) and the BAU (red dashed curves) and STA550 (green dashed curves) future scenarios. The smoothed thin curves are ensemble ranges whereas the thick curves are ensemble averages. The thick purple curve is observed surface temperature from Nicholls et al. (1996 and updates). The black curves are from a control run.

The ensemble-averaged, global-mean surface warming from 1990–99 to 2090–99 is ~1.9°C under the BAU scenario and ~1.5°C under the STA550 scenario (Fig. 1 shows the full time series). The BAU and STA550 warmings are very similar to those simulated by the CSM (Dai et al. 2001a). Interdecadal variations of the ensemble mean in Fig. 1 are, as one would expect, smaller than in the CSM single integration. The ensemble-mean temperatures under the BAU and STA550 scenarios start to diverge in the 2040s, but become significantly different only after the mid-2060s when the ensemble ranges no longer overlap (Fig. 1).

The ensemble range of the 20-yr smoothed global-mean temperature is ~0.25°C during 1870–1980 and becomes slightly smaller (~0.20°C) after 2050 (under both scenarios; Fig. 1). This ensemble range is similar to the peak-to-trough amplitude of 20-yr smoothed variations in the control run.[1] This result suggests that the ensemble uncertainty of coupled GCM simulations arises largely from the model's internal variability and that this uncertainty may be estimated using control run data.

The pattern of surface warming from 1961–90 to 2070–99 under the BAU scenario shows that the warming ranges between 1° and 2°C over the oceans and is above 2°C over many land areas, especially in northern high latitudes during winter where the warming is above 5°C (Fig. 2). (We use 30-yr mean here to reduce noise in the spatial patterns.) The ensemble-averaged spatial patterns of seasonal- and annual-mean surface warming are very similar under the BAU and STA550 scenarios with spatial correlation coefficients around 0.990. The spatial patterns (Fig. 2) are generally similar to those from other transient experiments using coupled GCMs forced by CO_2 or CO_2-plus-aerosol changes (Kattenberg et al. 1996; Mitchell et al. 1998; Roeckner et al. 1999; Boer et al. 2000; Dai et al. 2001a).

The PCM produces a moderate surface cooling (1°–2°C, mostly during winter) from 1961–90 to 2070–99 over the central midlatitude North Atlantic Ocean (Fig. 2). This cooling is larger at the ocean sur-

[1]The range shown in the control run over different time periods may be considered as a measure of the model's internal variability or the ensemble range of control runs since a long and stable control run can be sliced into several shorter (ensemble) runs.

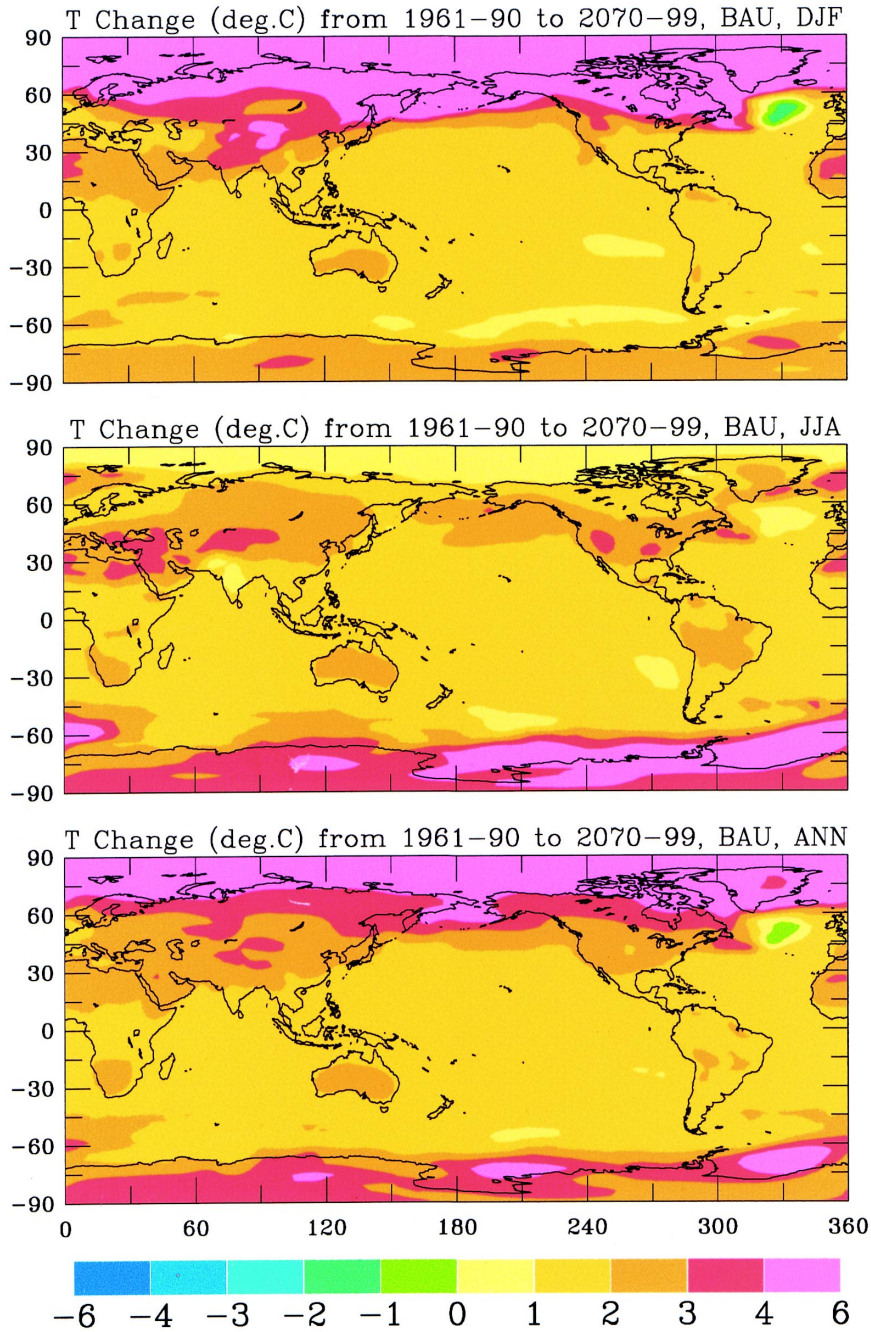

FIG. 2. Ensemble-averaged surface air temperature changes (°C) from 1961–90 to 2070–99 under the BAU scenario for (top) DJF, (middle) JJA, and (bottom) annual mean. Almost all the changes are statistically significant at the 5% level.

face than in the air (Fig. 3a). In most other similar model simulations, there is no such cooling, although the warming is often reduced over the northern North Atlantic compared to other regions. Two exceptions are the Goddard Institute for Space Studies (GISS) coupled model (Russell and Rind 1999) and HadCM3 (Wood et al. 1999). The GISS model showed 2°–4°C cooling over the North Atlantic and South Pacific and a 30% slowdown in the North Atlantic thermohaline circulation at the time of the doubling of atmospheric CO_2. A small surface cooling (~1.0°C) is also seen over the northern North Atlantic (associated with weakening of convection in the Labrador Sea) in one of the HadCM3 experiments at the time of CO_2 quadrupling.

Russell and Rind (1999) suggested that, in their model, the initial cause of the cooling is related to increased atmospheric poleward transport of latent heat energy and dry static energy, which leads to a reduction in the upward vertical fluxes of heat and moisture from the ocean surface at high latitudes. This stabilizes the ocean and reduces both convection (in the North Atlantic) and the strength of the thermohaline circulation. These changes result in less warm water brought up from below and less heat transport from the tropical Atlantic, causing the cooling over the North Atlantic.

In the PCM, the initial triggering cause for the cooling over the North Atlantic is different: it results from changes in the ocean circulation (Dai et al. 2001, manuscript to be submitted to Climate Dyn.), and atmospheric lapse rates over the region as greenhouse gas–induced radiative heating warms the free troposphere more than the surface (Fig. 4). The slower response of surface temperatures to the radiative forcing during the late twentieth and early twenty-first centuries (Figs. 3a and 4) results, in part, from rapid vertical mixing in the midlatitude North Atlantic. This oceanic mixing transports heat from the surface into the deep ocean and thus keeps surface temperatures relatively stable during the early stages of the greenhouse gas–induced warming (Fig. 3a). The free-tropospheric temperature, on the other hand, is not closely coupled with the sea surface temperature and rises fairly uniformly over northern midlatitudes in response to longwave radiative heating from increased water vapor (Fig. 4), CO_2, and other greenhouse gases.

The lapse rate changes initiate a complex series of processes. 1) By the 2040s, the change in lapse rates exceeds a threshold where the lower troposphere over the cooling region becomes so stable that atmospheric moist convection, as indicated by convective precipitation (Fig. 3b), surface sensible, and, more importantly, latent heat fluxes (Fig. 3c) begin to decrease rapidly. 2) This reduction in surface latent heat flux results in substantial decreases in net upward water flux (i.e., evaporation minus precipitation or *E–P*; Fig. 3c). 3) This reduces surface salinity from 1961–90 to 2070–99 over the cooling region by about 0.5–1.0 parts per thousand (not shown), which results in a 4%–8% decrease in the density of surface water (equivalent to the effect of a warming of about 3°–6°C; Pickard and Emery 1990, their p. 18). 4) This surface freshening, combined with freshening of coastal water due to melting of sea ice, decreases deep water formation in the North Atlantic and reduces the meridional overturning (i.e., the thermohaline circulation) in the North Atlantic sector by ~20% from 1961–90 to 2070–99 (Fig. 5; similar percentage changes for the global oceans). 5) This change in meridional overturning results in a reduction of northward heat transport from the tropical Atlantic to the midlatitude North Atlantic (Fig. 6, which also shows large decreases in northward heat transport in the tropical South Atlantic). For the zone from ~45° to 57°N (where the cooling occurs), there is net heat divergence in the surface layer (top 50 m) from 1961–90 to 2070–99 (i.e., there is an increase in the amount of heat being transported to the south and north; Fig. 6). 6) It is this heat divergence, combined with reduced local vertical mixing that causes the cooling over the midlatitude North Atlantic Ocean.

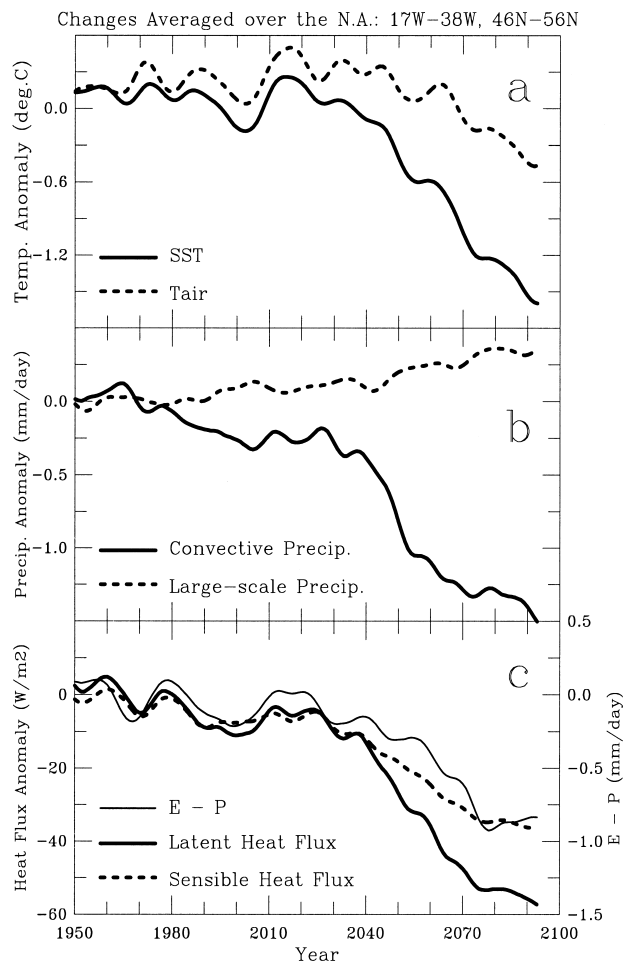

FIG. 3. Area-averaged anomalies (relative to the 1871–1999 mean) over the North Atlantic Ocean (46°–56°N, 17°–38°W): (a) surface air and sea temperature, (b) convective and large-scale precipitation, (c) surface latent and sensible heat flux (positive upward) and surface evaporation minus precipitation (*E–P*). All anomalies were averaged over five ensemble runs.

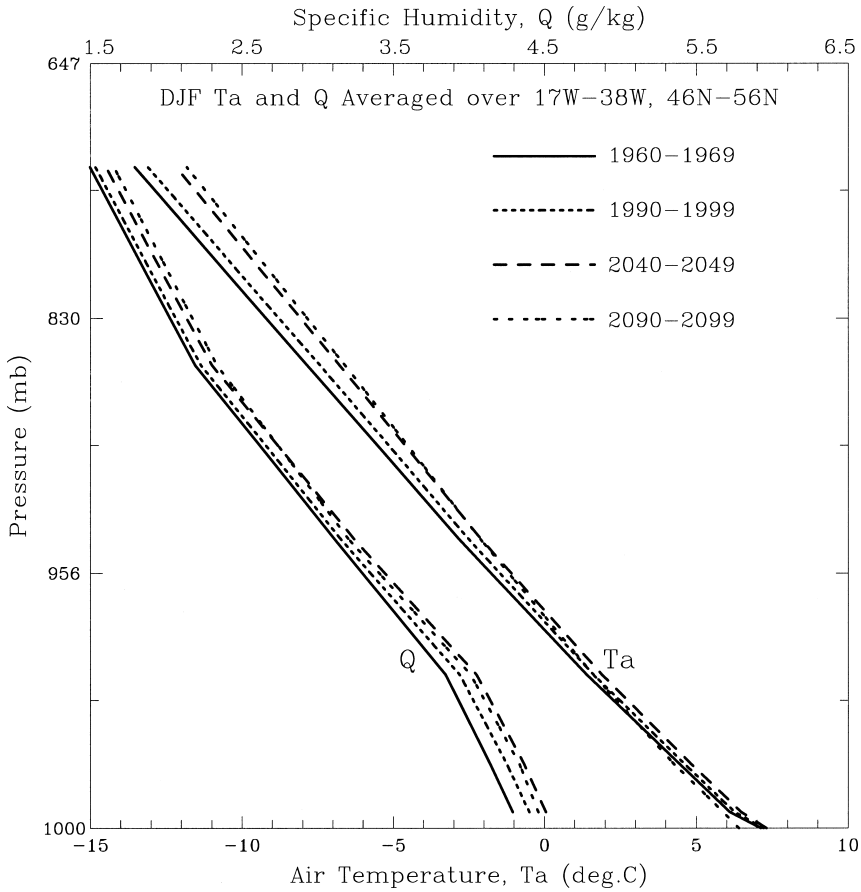

FIG. 4. Ensemble-averaged lower-tropospheric temperature (T_a) and specific humidity (Q) for DJF averaged over the midlatitude North Atlantic Ocean (46°–56°N, 17°–38°W) for 1960–69, 1990–99, 2040–49, 2090–99 (under the BAU scenario).

4. Precipitation, soil moisture, and cloud changes

Figure 7 shows that from 1990–99 to 2090–99 under the BAU scenario, global-mean precipitation increases from ~3.094 to ~3.195 mm day^{-1}, or by ~3.3%. Under the STA550 scenario, global-mean precipitation rises to only ~3.168 mm day^{-1}, or by 2.4%. The global-mean precipitation to temperature change ratio ($\Delta P / \Delta T$) is ~0.050 mm day^{-1} K^{-1}, or ~1.7% K^{-1}, for the 1990–2099 period under both scenarios. This may be compared with the average of 11 other models listed by Wigley (1999, his Table 2), which is 2.2% K^{-1} (range 1.1%–3.0% K^{-1}).

The ensemble range of the 20-yr smoothed global-mean precipitation rate is ~0.020 mm day^{-1} (0.7%) through the entire integration period for both scenarios (Fig. 7). This range is comparable to (although slightly larger than) the amplitude of the 20-yr smoothed variations in the control run. Again, this result suggests that intraensemble uncertainties may be approximated by internal variations in control runs. At the end of the runs, the ensemble ranges overlap only slightly, which suggests that the difference in the global-mean precipitation signals under the BAU and STA550 scenarios does not become statistically significant until late in the twenty-first century.

Regional precipitation changes can differ substantially among the ensemble runs, especially in the Tropics and subtropics and for seasonal precipitation. The regional patterns of ensemble-averaged precipitation changes are, however, very similar between the BAU and STA550 scenarios (with slightly smaller magnitudes for the STA550 case) (Fig. 8). The pattern correlation coefficients between the BAU and STA550 panels in Fig. 8 are 0.908 for December–January–February (DJF) and 0.943 for JJA. These values are substantially higher than those (0.572 and 0.841) found by Mitchell et al. (2000), who compared precipitation patterns from an ensemble of four integrations under a 1% CO_2 increase with those from single integrations under two different CO_2 stabilization scenarios. Our results show that ensemble-averaged simulations can provide reproducible estimates of regional precipitation changes and that lowering the rate of future CO_2 increases would not alter regional precipitation change patterns significantly.

In general, the ensemble-averaged precipitation in the BAU case shows a 20%–40% increase from 1961–90 to 2070–99 at high latitudes during winter (consistent with other models; Kattenberg et al. 1996) and a 10%–30% decrease over the subtropical dry areas (around 30° lat; Fig. 8). Other notable regional changes include a 20%–40% reduction in JJA precipitation in the western United States, a 20%–40% decrease in both DJF and JJA precipitation over the central midlatitude North Atlantic, and a 20%–40% increase in JJA precipitation over eastern Australia and over a

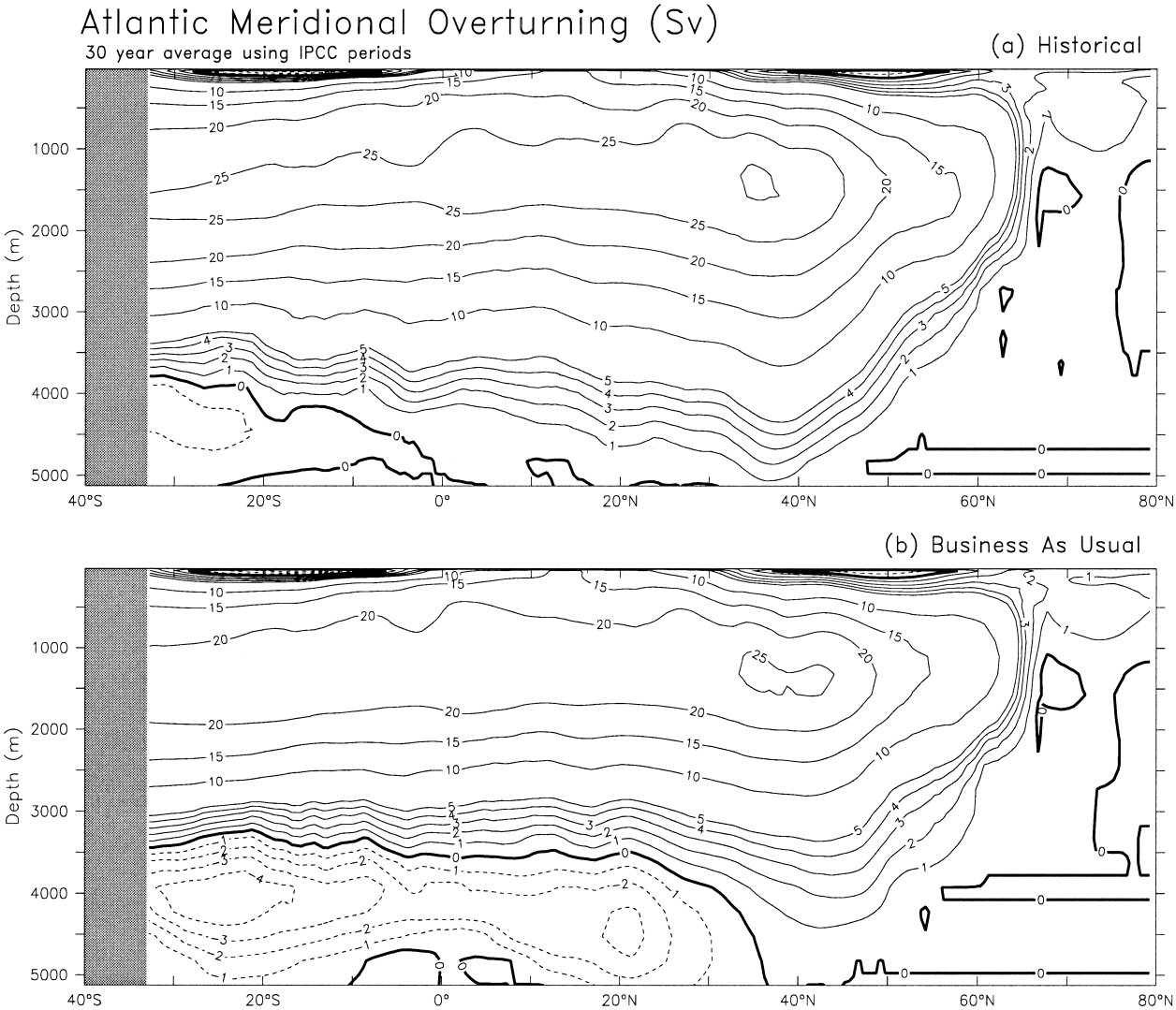

FIG. 5. Zonally averaged annual-mean meridional overturning streamfunction (Sv, 1 Sv = 10^6 m^3 s^{-1}) for the Atlantic sector for (a) 1961–90 in the historical run and (b) 2070–99 in the BAU case. Percentage changes are similar for seasonal plots. Five ensemble runs were used in the averaging.

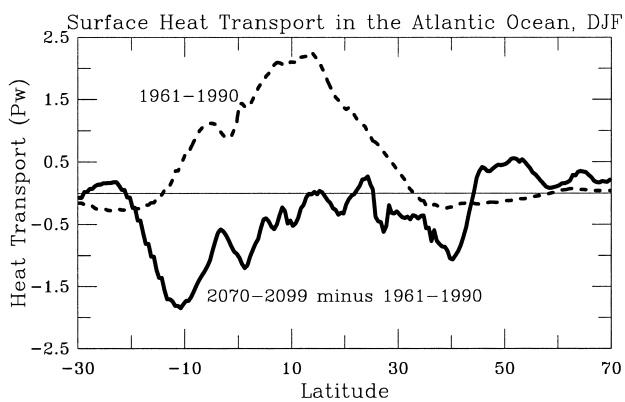

FIG. 6. Zonally averaged meridional heat transport within the top 50 m in the Atlantic Ocean for 1961–90 (dashed line) and the change of this transport from 1961–90 to 2070–99 (solid line). Note that the 1960–90 mean transport is in units of Pw (1 Pw = 10^{15} watts) while the change is in units of 0.1 Pw. Five ensemble runs were used in the averaging.

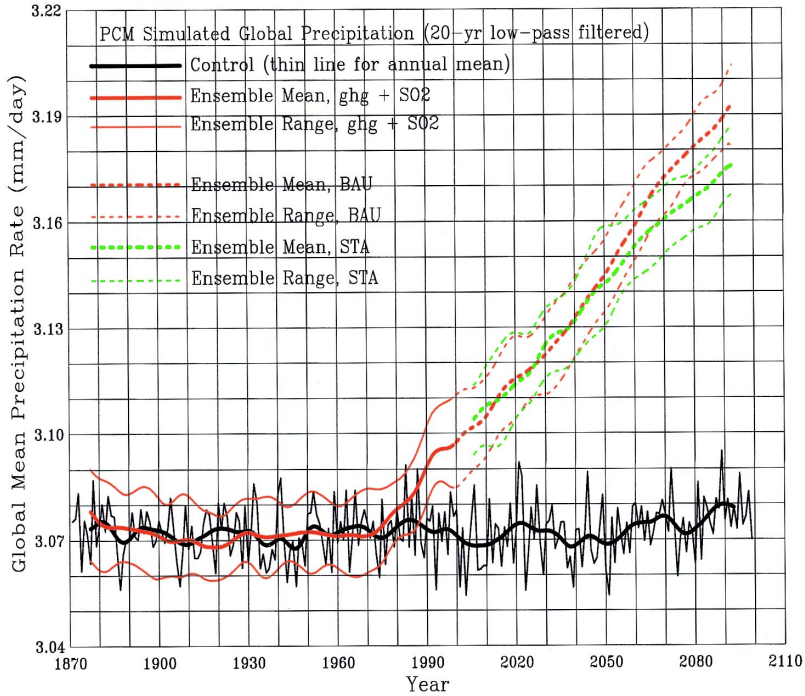

FIG. 7. Same as Fig. 1 but for precipitation (with no observation).

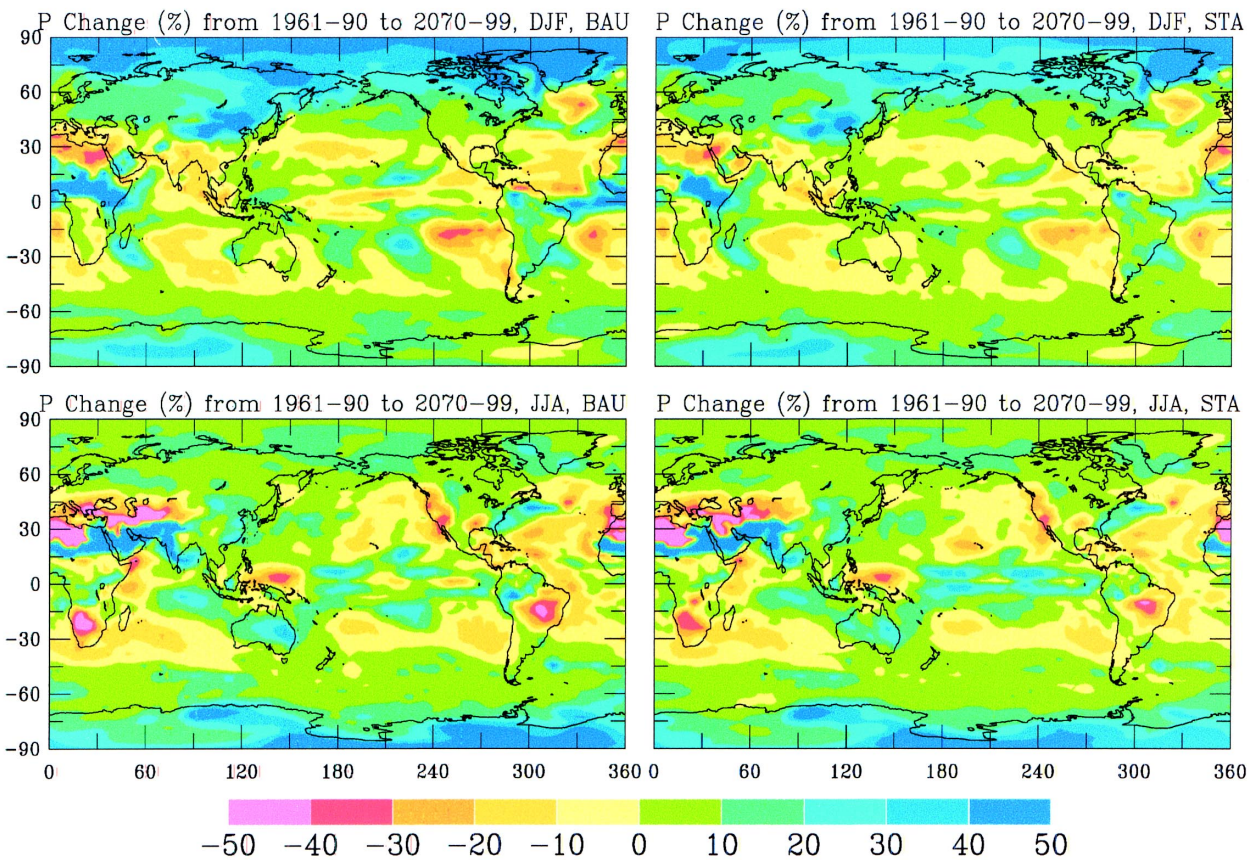

FIG. 8. Ensemble-averaged precipitation changes (%) from 1961–90 to 2070–99 under the (left) BAU and (right) STA550 scenarios for (upper) DJF and (lower) JJA. Changes within ±10% are not significant statistically.

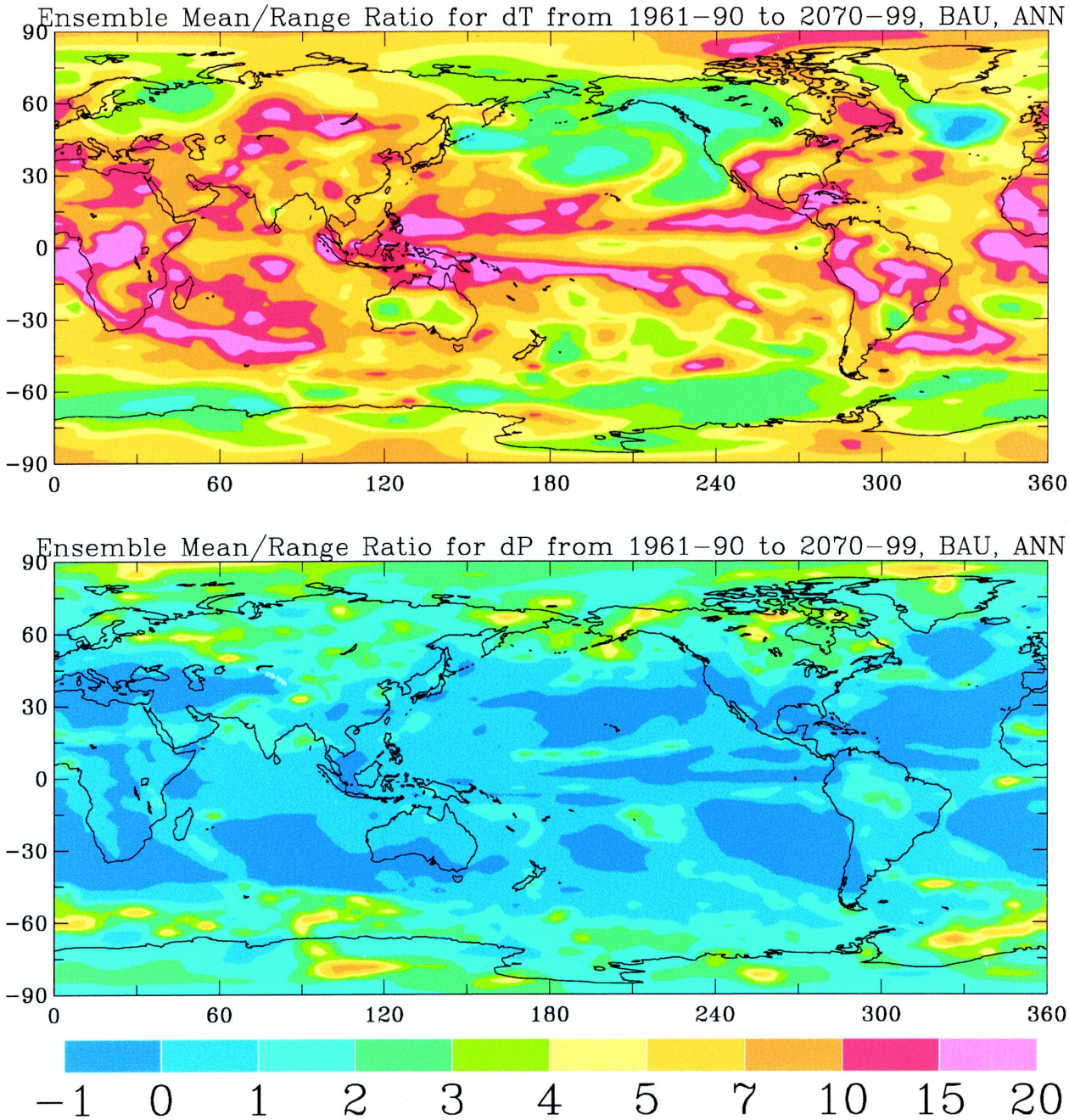

FIG. 9. Ensemble mean to ensemble range ratio for (upper) annual surface temperature and (lower) precipitation changes from 1961–99 to 2070–99 simulated by the PCM under the BAU scenario.

region including western India, Saudi Arabia, and Egypt (Fig. 8). Similar, but slightly smaller changes occur in the STA ensemble mean.

The intraensemble variability at the gridbox level can, however, be large even for annual-mean values of temperature and precipitation. For example, annual temperature changes can differ by 2°–3°C over the sea-ice areas at northern high latitudes among ensemble members (≥5°C for DJF temperature changes, not shown).

Figure 9 shows a signal-to-noise ratio for annual-mean temperature and precipitation changes from 1961–90 to 2070–99 defined by ensemble mean over ensemble range. This ratio is roughly 0.404 times the ratio of ensemble mean over intraensemble standard deviation (assuming a Gaussian distribution). It provides a guide to the statistical significance of the simulated changes—a value above 0.79 corresponds to a mean-to-standard deviation ratio above 1.96 and thus

is statistically significant at the 5% level. Under the BAU scenario, the mean-to-range ratio for temperature change exceeds 4 over most areas except for regions with large variability (e.g., due to sea ice). This signal-to-noise ratio is highest in the Tropics due to small intraensemble variability there. On the other hand, the ratio for precipitation is highest (~1–7) at mid- and high latitudes (Fig. 9) because of the small variability and large changes for precipitation at these latitudes.

Soil moisture changes in the BAU ensemble mean (from 1961–90 to 2070–99) are generally small (±3%) over most areas, with a 2%–10% decrease over Europe and western Asia, Canada, and Alaska; a 5%–10% increase over eastern China during JJA; a 2%–5% increase in northern mid- and high latitudes; and a 2%–10% decrease over the southern United States and southeastern Australia during DJF (not shown). Changes in the STA550 case are similar to these over many areas.

Total cloud-cover changes are within ±5% (of sky cover) over most regions in both the BAU and STA550 ensemble means, with a 2%–6% decrease over northern mid- and high latitudes during DJF, and a 2%–6% increase over northern high latitudes, eastern Asia, and the tropical Indian Ocean during JJA. Mid-level clouds decrease while high-level clouds increase, as in previous GCM experiments (Kattenberg et al. 1996).

5. Discussion and summary

Ensemble averaging reduces the noise level in model-simulated climate changes, especially on regional and smaller scales. However, the results of this study still contain uncertainties resulting from model deficiencies in simulating the climate response to any given forcing and from uncertainties in future emissions. The PCM has a climate sensitivity of ~2.1°C global-mean warming for a doubling of atmospheric CO_2. This sensitivity, which is in the lower half of the 1.5°–4.5°C range of most GCMs (Kattenberg et al. 1996), largely determines the magnitude of the simulated global-mean warming by the end of twenty-first century. It should be noted that the simulated global warming over 1870–2099 is only ~70%[2] of the total warming that will eventually occur due to the forcing over this period. This percentage is somewhat higher than that (~50%) in the GFDL model (with 1% yr^{-1} CO_2 forcing), which has a much higher climate sensitivity (~4.5°C) (Stouffer and Manabe 1999). The difference here is consistent with the known dependence on the climate sensitivity of the fraction of warming that is realized in time-dependent forcing simulations (see, e.g., Wigley and Schlesinger 1985).

As already noted, reduced levels of CO_2 reduce the magnitude of the simulated changes (by the end of the twenty-first century) only moderately[3] with no significant differences in spatial and seasonal patterns of change for both temperature and precipitation. Compared with the BAU case, the surface warming under the STA550 scenario is reduced by a few tenths of a degree over the oceans and tropical land areas, and by 0.5°–1.0°C over mid- and high-latitude land areas. These reductions are somewhat smaller than those obtained by Mitchell et al. (2000), partly because their simulations had higher forcing differences, and partly because their model has a higher climate sensitivity (2.5°C compared with 2.1°C for the PCM). Mitchell et al.'s results also show similar patterns of change in the BAU and stabilization scenarios, but the similarities are far less clear than in our simulations. This may reflect the fact that they used only single realizations for their stabilization runs.

Over the central midlatitude North Atlantic, there is a moderate surface cooling (1°–2°C, mostly during winter) from 1961–90 to 2071–99. This cooling is triggered by changes in the ocean circulation and atmospheric lapse rates over the region (i.e., larger warming in the free troposphere than at the surface), which decreases surface evaporation and salinity and thus stabilizes the surface ocean. The resultant reduction in local oceanic convection contributes to a 20% slowdown in the thermohaline circulation and a heat divergence in the top 50-m layer of the ocean over the cooling region.

If the climate changes obtained here are realistic, our results show that the global warming trend since

[2]This number was estimated as follows. The equilibrium or total warming for a doubling of CO_2 is ~2.1°C with a radiative forcing of ~3.5 W m^{-2} (Meehl et al. 2000a). The radiative forcing from 1870 to 2099 is ~6.0 W m^{-2} (Dai et al 2001a), so the equilibrium warming for this forcing is about $6.0 \times (2.1/3.5) = 3.6$°C. The realized warming from 1870 to 2099 is ~2.5°C (Fig. 1) or ~69% of the equilibrium warming.

[3]The warming difference is, however, likely to increase substantially if the CO_2 trends of the two scenarios continue into the twenty-second century (Dai et al. 2001c).

the late 1970s (see, e.g., Wigley 2000) is likely to continue through much of the twenty-first century. Efforts to stabilize atmospheric CO_2 concentration at ~550 ppm will only slow down the warming moderately, and the slowdown will only become apparent in the mid-twenty-first century. Global precipitation under the BAU scenario is likely to increase by ~3% during the next 100 yr, with the largest (percentage) increases over northern mid- and high-latitudes during winter. Soil moisture changes by the end of the twenty-first century are generally small (±3%) over most areas. The CO_2 stabilization reduces these changes by only small amounts.

Acknowledgments. J. W. Weatherly, T. W. Bettge, W. G. Strand, V. B. Wayland, and A. P. Craig contributed to the PCM simulations, and J. T. Kiehl and B. A. Boville provided sulfate loading data. We also thank Kevin E. Trenberth, Benjamin D. Santer, and Karl E. Taylor for their constructive comments. The PCM simulations were supported by the U.S. Department of Energy and U.S. National Science Foundation (NSF). The input concentration scenarios were developed under the ACACIA program, funded by EPRI, CRIEPI, KEMA, and NCAR.

References

Allen, M. R., P. A. Stott, J. F. B. Mitchell, R. Schnur, and T. L. Delworth, 2000: Quantifying the uncertainty in forecasts of anthropogenic climate change. *Nature,* **407,** 617–620.

Boer, G. J., Flato, and D. Ramsden, 2000: A transient climate change simulation with greenhouse gas and aerosol forcing: projected climate for the 21 century. *Climate Dyn.,* **16,** 427–450.

Cubasch, U., K. Hasselmann, H. Höck, E. Maier-Reimer, U. Mikolajewicz, B. D. Santer, and R. Sausen, 1992: Time-dependent greenhouse warming computations with a coupled ocean–atmosphere model. *Climate Dyn.,* **8,** 55–69.

——, and Coauthors, 1994: Monte Carlo climate forecasts with global coupled ocean–atmosphere model. *Climate Dyn.,* **10,** 1–19.

Dai, A., T. M. L. Wigley, B. A. Boville, J. T. Kiehl, and L. E. Buja, 2001a: Climates of the twentieth and twenty-first centuries simulated by the NCAR Climate System Model. *J. Climate,* **14,** 485–519.

——, G. A. Meehl, W. M. Washington, and T. M. L. Wigley, 2001b: Climate changes in the 21st century over the Asia-Pacific region simulated by the NCAR CSM and PCM. *Adv. Atmos. Sci.,* **18,** 639–658.

——, T. M. L. Wigley, G. A. Meehl, and W. M. Washington, 2001c: Effects of stabilizing atmospheric CO_2 on global climate in the next two centuries. *Geophys. Res. Lett.,* in press.

Delworth, T. L., and T. R. Knutson, 2000: Simulation of early 20th century global warming. *Science,* **287,** 2246–2250.

Edmonds, J., M. Wise, H. Pitcher, R. Richels, T. M. L. Wigley, and C. MacCracken, 1997: An integrated assessment of climate change and the accelerated introduction of advanced energy technologies: An application of MiniCAM 1.0. *Mitigat. Adapt. Strategies Global Change,* **1,** 311–339.

Hansen, J., and coauthors, 1997: Forcings and chaos in interannual to decadal climate change. *J.Geophys. Res.,* **102,** 25 679–25 720.

Kattenberg, A., and Coauthors 1996: Climate models—Projections of future climate. *Climate Change 1995*: *The IPCC Second Assessment,* J. T. Houghton et al., Eds., Cambridge University Press, 285–358.

Manabe, S., R. J. Stouffer, M. D. Spelman, and K. Bryan, 1991: Transient response of a coupled ocean–atmosphere model to gradual changes of atmospheric CO_2. Part I: Annual mean response. *J. Climate,* **4,** 785–818.

Meehl, G. A., W. D. Collins, B. Bonville, J. T. Kiehl, T. M. L. Wigley, and J. M. Arblaster, 2000a: Response of the NCAR Climate System Model to increased CO_2 and the role of physical processes. *J. Climate*, **13,** 1879–1898.

——, G. J. Boer, C. Covey, M. Latif, and R. J. Stouffer, 2000b: The Coupled Model Intercomparison Project (CMIP). *Bull. Amer. Meteo. Soc.,* **81,** 313–318.

——, P. R. Gent, J. M. Arblaster, B. Otto-Bliesner, E. C. Brady, and A. P. Craig, 2001: Factors that affect amplitude of El Niño in global coupled climate models. *Climate Dyn.,* **17,** 515–526.

Mitchell, J. F. B., T. C. Johns, J. M. Gregory, and S. F. B. Tett, 1995: Climate response to increasing levels of greenhouse gases and sulfate aerosols. *Nature*, **376,** 501–504.

——, and C. A. Senior, 1998: Transient response to increasing greenhouse gases using models with and without flux adjustment. Hadley Centre for Climate Prediction and Research Tech. Note 2, 15 pp.

——, W. J. Ingram, and J. A. Lowe, 2000: The effect of stabilizing atmospheric carbon dioxide concentration on global and regional climate change. *Geophys. Res. Lett.*, **27,** 2977–2980.

Nakićenović, N., and R. Swart, Eds., 2000: *IPCC Special Report on Emission Scenarios.* Cambridge University Press, 570 pp.

Nicholls, N., G. V. Gruza, J. Jouzel, T. R. Karl, L. A. Ogallo, and D. E. Parker, 1996: Observed climate variability and change. *Climate Change 1995: The IPCC Second Assessment,* J. T. Houghton et al., Eds., Cambridge University Press, 133–192.

Pickard, G. L., and W. J. Emery, 1990: *Descriptive Physical Oceanography: An Introduction,* 5th ed. Pergamon Press, 320 pp.

Roeckner, E., L. Bengtsson, J. Feichter, J. Lelieveld, and H. Rodhe, 1999: Transient climate change simulations with a coupled atmosphere–ocean GCM including the tropospheric sulfur cycle. *J. Climate,* **12,** 3004–3032.

Rowell, D. P., 1998: Assessing potential seasonal predictability with an ensemble of multidecadal GCM simulations. *J. Climate*, **11,** 109–120.

Russell, G. L., and D. Rind, 1999: response to CO_2 transient increase in the GISS coupled model: Regional coolings in a warming climate. *J. Climate*, **12,** 531–539.

Stott, P. A., S. F. B. Tett, G. S. Jones, M. R. Allen, J. F. B. Mitchell, and G. J. Jenkins, 2000: External control of 20th century temperature by natural and anthropogenic forcings. *Science,* **290,** 2133–2137.

——, ——, ——, ——, W. J. Ingram, and J. F. B. Mitchell, 2001: Attribution of twentieth century temperature change to natural and anthropogenic causes. *Climate Dyn,*. **17,** 1–21.

Stouffer, R. J., and S. Manabe, 1999: Response of a coupled ocean–atmosphere model to increasing atmospheric carbon

dioxide: Sensitivity to the rate of increase. *J. Climate*, **12,** 2224–2237.

Washington, W. M., and Coauthors, 2000: Parallel Climate Model (PCM) control and transient simulations. *Climate Dyn.*, **16,** 755–774.

Wehner, M. F., 2000: A method to aid in the determination of the sampling size of AGCM ensemble simulations. *Climate Dyn.*, **16,** 321–331.

Wigley, T. M. L., 1999: *The Science of Climate Change*: *Global and U.S. Perspectives*, Pew Center on Global Climate Change, 48 pp.

——, 2000: ENSO, volcanoes and record-breaking temperatures. *Geophys. Res. Lett.*, **27,** 4101–4104.

——, and M. E. Schlesinger, 1985: Analytical solution for the effect of increasing CO_2 on global-mean temperature. *Nature*, **315,** 649–652.

——, R. Richels, and J. A. Edmonds, 1996: Economic and environmental choices in the stabilization of atmospheric CO_2 concentrations. *Nature*, **379,** 240–243.

Wood, R. A., A. B. Keen, J. F. B. Mitchell, and J. M. Gregory, 1999: Changing spatial structure of the thermohaline circulation in response to atmospheric CO_2 forcing in a climate model. *Nature*, **399,** 572–575.

Zwiers, F. W., 1996: Interannual variability and predictability in an ensemble of AMIP climate simulations conducted with the CCC GCM2. *Climate Dyn.*, **12,** 825–847.